

Impact of different eddy covariance sensors, site set-up, and maintenance on the annual balance of CO₂ and CH₄ in the harsh Arctic environment



J.P. Goodrich^{a,*}, W.C. Oechel^{a,b}, B. Gioli^c, V. Moreaux^{a,d}, P.C. Murphy^a, G. Burba^e, D. Zona^{a,f}

^a Global Change Research Group, Dept. of Biology, San Diego State University, San Diego, CA, 92182, USA

^b Department of Environment, Earth, and Ecosystems, The Open University, Milton Keynes, England, MK7 6AA, UK

^c IBIMET-CNR, Istituto di Biometeorologia, Consiglio Nazionale delle Ricerche, Via G. Caproni 8, 50145 Firenze, Italy

^d Now at: INRA, UMR 1137, Forest Ecology and Ecophysiology, Centre de Nancy, F-54280 Champenoux, France

^e Science & Technology, LI-COR Biosciences, 4421 Superior St., Lincoln, NE, 68504, USA

^f Dept. of Animal and Plant Sciences, University of Sheffield, Western Bank, Sheffield, S10 2TN, UK

ARTICLE INFO

Article history:

Received 11 September 2015

Received in revised form 28 June 2016

Accepted 10 July 2016

Keywords:

Arctic

Eddy covariance

Open-path

Closed-path

Sonic anemometer

ABSTRACT

Improving year-round data coverage for CO₂ and CH₄ fluxes in the Arctic is critical for refining the global C budget but continuous measurements are very sparse due to the remote location limiting instrument maintenance, to low power availability, and to extreme weather conditions. The need for tailoring instrumentation, site set up, and maintenance at different sites can add uncertainty to estimates of annual C budgets from different ecosystems. In this study, we investigated the influence of different sensor combinations on fluxes of sensible heat, CO₂, latent heat (LE), and CH₄, and assessed the differences in annual CO₂ and CH₄ fluxes estimated with different instrumentation at the same sites. Using data from four sites across the North Slope of Alaska, we found that annual CO₂ fluxes estimated with heated ($7.5 \pm 1.4 \text{ gC m}^{-2} \text{ yr}^{-1}$) and non-heated ($7.9 \pm 1.3 \text{ gC m}^{-2} \text{ yr}^{-1}$) anemometers were within uncertainty bounds. Similarly, despite elevated noise in 30-min flux data, we found that summer CO₂ fluxes from open ($-17.0 \pm 1.1 \text{ gC m}^{-2} \text{ yr}^{-1}$) and close-path ($-14.2 \pm 1.7 \text{ gC m}^{-2} \text{ yr}^{-1}$) gas analyzers were not significantly different. Annual CH₄ fluxes were also within uncertainty bounds when comparing both open ($4.5 \pm 0.31 \text{ gC m}^{-2} \text{ yr}^{-1}$) and closed-path ($4.9 \pm 0.27 \text{ gC m}^{-2} \text{ yr}^{-1}$) gas analyzers as well as heated ($3.7 \pm 0.26 \text{ gC m}^{-2} \text{ yr}^{-1}$) and non-heated ($3.7 \pm 0.28 \text{ gC m}^{-2} \text{ yr}^{-1}$) anemometers. A continuously heated anemometer increased data coverage (64%) relative to non-heated anemometers (47–52%). However, sensible heat fluxes were over-estimated by 12%, on average, with the heated anemometer, contributing to the overestimation of CO₂, CH₄, and LE fluxes (mean biases of $-0.03 \mu\text{mol m}^{-2} \text{ s}^{-1}$, $-0.05 \text{ mgC m}^{-2} \text{ h}^{-1}$, and -3.77 W m^{-2} , respectively). To circumvent this potential bias and reduce power consumption, we implemented an intermittent heating strategy whereby activation only occurred when ice or snow blockage of the transducers was detected. This resulted in comparable coverage (50%) during winter to the continuously heated anemometer (46%), while avoiding flux over-estimation. Closed and open-path analyzers showed good agreement, but data coverage was generally greater when using closed-path, especially during winter. Winter data coverage of 26–32% was obtained with closed-path devices, vs 10–14% for the open-path devices with unheated anemometers or up to 46% and 35% using closed and open-path analyzers, respectively with heated anemometers. Accurate estimation of LE remains difficult in the Arctic due to strong attenuation in closed-path systems, even when intake tubes are heated, and due to poor data coverage from open-path sensors in such a harsh environment.

© 2016 Elsevier B.V. All rights reserved.

1. Introduction

Assessment of Arctic ecosystem-atmosphere carbon (C) exchange is critical for refining the global C budget (IPCC, 2007; Fisher et al., 2014). Despite the importance of both CO₂ and CH₄

* Corresponding author.

E-mail address: jpgoodrich@mail.sdsu.edu (J.P. Goodrich).

emissions from the Arctic and their sensitivity to climate change (Mastepanov et al., 2013; Ueyama et al., 2013), their annual balances are still largely uncertain (Melton et al., 2013; Fisher et al., 2014). Although some researchers have had success measuring ecosystem-scale Arctic CO₂ and CH₄ fluxes (Oechel et al., 2014; Kutzbach et al., 2007; Parmentier et al., 2011; Emmerton et al., 2015; Zona et al., 2014, 2016), spatial and temporal data coverage is still sparse and year-round coverage is especially lacking (Wille et al., 2008; Oechel et al., 2014; Euskirchen et al., 2012; Lüers et al., 2014). The scarcity of continuous, year-round measurements in the Arctic is due to the extremely harsh environmental conditions, especially in winter, and relative lack of infrastructure in these remote sites, preventing regular maintenance of the instruments or making it prohibitively expensive. These challenges have limited our ability to obtain accurate annual C budgets and assess interannual variability in greenhouse gas fluxes from Arctic regions.

Currently, important scientific questions on the terrestrial C cycle are based on multi-site syntheses of flux data from eddy covariance tower networks (e.g. FLUXNET, AmeriFlux, ICOS, AsiaFlux). Although there are ongoing efforts to standardize the sensors used in these networks (i.e. ICOS, NEON, etc.), a variety of different instruments, and site-dependent processing methods are still employed (Fratini et al., 2014). In addition, as technology improves and new sensor models become available, instrumentation is often upgraded after years of field deployment at long-term sites (e.g., Burns et al., 2014). Such methodological and instrumental differences and updates may contribute to observed differences in seasonal and annual C budgets, and add uncertainty when comparing C fluxes from different sites or ecosystems, as well as among years at long-term sites. Bias in measurements due to instrumentation changes becomes particularly important in the Arctic where C fluxes can be very small (especially in winter), and can be considerably influenced by post-processing corrections (Oechel et al., 2014).

Additionally, the configuration of gas analyzers and sonic anemometers at a given site often needs to be tailored to the specific requirements of that environment and available infrastructure, and therefore may vary in different sites even across standardized networks (e.g. the boreal sites in ICOS will need to rely on heated sonic anemometers, which will not be needed in the more southern sites). With respect to gas analyzers, both open- and closed-path sensors have been deployed worldwide for CO₂ and H₂O flux measurements, and both have shown good performance in the Arctic (Nakai et al., 2011, 2013; Oechel et al., 2014; Zona et al., 2016). Multiple studies have compared open-path and closed-path analyzers in different conditions for CO₂ fluxes (Leuning and King, 1992; Lee et al., 1994; Järvi et al., 2009; Ueyama et al., 2012; Burns et al., 2014). Open-path analyzers typically require less overall maintenance, have considerably smaller power demand, better time response and smaller frequency corrections than closed-path systems due to the absence of pumps, filters, and intake tubes (Massman, 1991, 2000). However, they require larger corrections for density fluctuations (Webb-Pearman-Leuning correction, WPL, Webb et al., 1980), and older models may need surface heating corrections, particularly during winter (Grelle and Burba, 2007; Burba et al., 2008; Oechel et al., 2014). Open-path sensors also lose more data during precipitation and under high humidity or fog (Järvi et al., 2009). The annual data coverage of closed-path systems in harsh environments has been up to 70% (Goulden et al., 2006), while open-path designs resulted in overall annual data coverage of 44–68% (Oechel et al., 2014; Euskirchen et al., 2012) but as low as 15% during winter (Oechel et al., 2014). Increased maintenance frequency or winterization of the instrument can increase open-path data coverage, but these are often costly or impractical.

For CH₄ flux measurements, successful inter-comparisons of open-path and closed-path analyzers have also been performed (Detto et al., 2011; Peltola et al., 2013; Iwata et al., 2014). While the open-path design (LI-7700) can lead to substantial data losses due to precipitation, with data coverage as low as 25% in the harsh Arctic environment (Sturtevant et al., 2012), it is usually the only option for CH₄ flux measurements at remote sites due to low power consumption and autonomous operation (McDermitt et al., 2011; Burba, 2013). Furthermore, this sensor was successfully deployed in an alpine wetland (mean annual temperature = −1.1 °C) attaining data coverage up to 66% (Song et al., 2015). Generally, closed-path systems have better data coverage in the Arctic with 66–85% (Zona et al., 2016, 2009; Sachs et al., 2008), although depending on the set-up and maintenance schedule, associated technical and power supply issues can reduce closed-path data capture to 12–26% in Arctic and sub-Arctic sites (Hanis et al., 2013; Wille et al., 2008).

Various sonic anemometers have been used extensively in cold environments (Gažovič et al., 2013; Jackowicz-Korcynski et al., 2010; Sturtevant et al., 2012; Zona et al., 2009, 2010; Rinne et al., 2007), but a major challenge for measuring fluxes in these regions is anemometer performance in extreme weather conditions when water, snow, and ice can block or divert the sonic signals from the transducers. In order to measure fluxes outside the summer period, the transducers of the sonic anemometer need to be maintained ice-free. Heating systems for these sensors have generally utilized heating tape wrapped around the anemometer and, less commonly, the hot film technology (Lekakis et al., 1989; Skelly et al., 2002). Since it has been shown that continuous heating of the anemometer may increase the apparent sensible heat fluxes (Tammelin et al., 1998; Skelly et al., 2002), an intermittent heating strategy needs to be explored at cold sites. Although multiple cross-comparisons of sonic anemometers have been performed in the past (e.g. Kochendorfer et al., 2012; Frank et al., 2013; El-Madany et al., 2013; Nakai et al., 2014), none have yet tested the impact of heating on the sensible heat and gas fluxes in Arctic sites. One of the few commercially available self-heating anemometers is provided by Metek GmbH (uSonic-3 Class A), which initiates heating based on air temperature thresholds, whereby the heater is maintained on for temperatures below 4.5 °C. In the Arctic, this temperature-activated heating would result in continuous heating for the entire autumn, winter and spring, potentially affecting the fluxes during the most critical and uncertain periods, emphasizing the need for a better heating strategy.

To investigate how the choice of gas analyzers and sonic anemometers influences fluxes of CO₂ (F_{CO_2}), latent heat (LE), sensible heat (H), and CH₄ (F_{CH_4}) and to understand the potential influence of different configurations on the long term C budget, we compared several recently installed instrument sets to the historically operating sets at four flux sites in Arctic Alaska. Instrument configuration at each site was selected depending on availability of line power, climate conditions, and site accessibility. This study reports on the comparability over half-hourly scales for F_{CO_2} , LE, H, and F_{CH_4} , and on annual totals of F_{CO_2} and F_{CH_4} . The comparisons are organized as follows:

- i) Comparisons of fluxes derived from heated and non-heated anemometers from half-hourly (all fluxes) to annual time scales (for F_{CO_2} and F_{CH_4}).
- ii) Comparisons of F_{CO_2} and LE obtained from closed-path and (en)closed-path analyzers.
- iii) Comparisons of F_{CO_2} , and F_{CH_4} obtained from open-path and closed-path analyzers.

In addition to direct comparisons of final fluxes, we investigated the influence of site and sensor specific spectral corrections, which are known to vary greatly depending on the site (e.g., Ibrom et al.,

2007; Leuning and King, 1992). The results of this study should provide useful and practical considerations for future studies as well as for ongoing instrumental updates at long-term measurement sites. These may be particularly helpful for experimental design, station setup, configuration and maintenance planning, as well as data interpretation at other remote, high-latitude, cold sites experiencing long periods of small C fluxes.

2. Materials and methods

2.1. Study sites

The eddy covariance (EC) flux towers were located at four sites on the North Slope of Alaska: two in Barrow (CMDL and BES), one in Atkasuk (ATQ) and one in Ivotuk (IVO). The CMDL site (71°19′21.10″ N; 156°36′33.04″ W, 1 m elevation above sea level) is about 2 km south of the Arctic Ocean. This wet sedge tundra site is characterized by low species diversity, dominance of grasses and sedges, rare occurrences of tussock, and a lack of shrubs (Brown et al., 1980). Further site details can be found in Kwon et al. (2006). The BES site is 6.5 km south of the Arctic Ocean (71°16′51.17″ N, 156°35′47.28″ W, 3 m elevation), and dominant vegetation includes grasses, sedges, and mosses along with a few prostrate dwarf shrubs (Mullier et al., 1999; Reynolds et al., 2005; Zona et al., 2011). More site details are available in Zona et al. (2012). Both CMDL and BES are located near Barrow, have grid power and relatively easy access for instrumentation maintenance including during the winter. The ATQ site (70°28′10.64″ N; 157°24′32.21″ W, 24 m elevation) is located approximately 100 km south of Barrow, also has access to line power, and is fairly accessible during the winter. This site is characterized by moist coastal sedge tundra with moist-tussock vegetation (Kwon et al., 2006). More information can be found in Oechel et al. (2014). The IVO site (68°29′11.36″ N; 155°45′0.79″ W, 543 m elevation) is located approximately 300 km south of Barrow, at the foothills of the Brooks Mountain Range. Dominant vegetation includes tussock species, dwarf and creeping shrubs, mosses and lichen. More site information is provided in Zona et al. (2016). This site does not have line power access and thus is powered by combination of two diesel generators, twelve solar panels, and a wind turbine. Access to IVO requires chartered flights to a remote air strip, limiting instrument maintenance to the summer period only.

2.2. Long-term instrumentation at study sites

The initial selection of instrumentation at each site was made largely based on the need to limit maintenance and servicing of the sensors as well as on power restrictions. We also endeavored to deploy the most appropriate instrumentation commercially available at the time of each set-up (spanning approximately 15 years). This necessitated different instrument configurations over time as well as among the sites (Table 1).

The CMDL site, established in 1997, was upgraded with an LI-7500 CO₂/H₂O analyzer in 2001 and with a Gill WindMaster Pro in 2012. The LI-7500 was then replaced by the (en)closed-path LI-7200 (Burba et al., 2010, 2012) gas analyzer in 2011, and an open-path LI-7700 CH₄ analyzer was installed in 2013. BES was established in summer 2005, and was initially equipped with a Gill WindMaster Pro anemometer and open-path LI-7500 CO₂/H₂O analyzer (Zona et al., 2012). ATQ was established in 1999, initially equipped with a Gill R3 anemometer and updated with an open-path LI-7500 CO₂/H₂O analyzer in 2001. The gas analyzer was then replaced by an (en)closed-path LI-7200 in 2011. The IVO site was first installed in 2003 and included an LI-7500 gas analyzer and Gill R3 anemometer. Data acquisition was nearly continuous at

all of these sites, except IVO where data collection was stopped in summer 2008 and re-started in summer 2013. In all sites, new instrument models were added in summer/fall 2013 as described below. Data from October 2013 to July 2015 were used for the comparisons of sonic anemometers and gas analyzers in this study.

2.3. Instrumentation for sensor comparison

In 2013, a Metek uSonic-3 Class A non-orthogonal ultrasonic anemometer with self-heating feature (hereafter referred to as Metek) and a CSAT3 anemometer (non-orthogonal) were installed at ATQ for comparison along with the non-orthogonal Gill R3. At ATQ, the Metek was heated continuously until March 2015, when the heating was switched off, whereas both the Gill R3 and CSAT3 were not heated (Table 1).

At the remote IVO site, a Metek anemometer was also deployed in 2013. To limit power consumption, we developed an intermittent heating strategy such that heating was activated only when the transducers were blocked as reported by analog data quality indicators, rather than the default activation scheme based on the sonic temperature. The impact of this power-efficient heating strategy was investigated with respect to its effectiveness for de-icing the anemometer, the resulting data coverage during cold-periods, and the quality of sensible heat flux measurements.

As part of a larger effort toward upgrading instrumentation, we installed closed-path LGR-FGGA-24EP CO₂/H₂O/CH₄ analyzers at the CMDL, BES, and ATQ sites. To assess data continuity and comparability, we compared CO₂ and LE fluxes from the LGR-FGGA-24EP at ATQ to those from the (en)closed-path LI-7200 system (Table 1). At BES, the CO₂ fluxes from the LGR-FGGA-24EP were compared to those from the open-path LI-7500 (Table 1). Due to condensation issues within the long inlet tube at BES (the wettest, inundated site), the signal lag between vertical wind and H₂O vapor concentrations became very large and insurmountable for spectral corrections. LE fluxes therefore, could not be used from the LGR-FGGA-24EP for direct comparison with the LI-7500 at that site. Finally, at CMDL, CH₄ fluxes from the LGR-FGGA-24EP were compared to those measured by the open-path LI-7700 analyzer (Table 1).

2.4. Instrumentation set-up

At ATQ, the LI-7200 analyzer utilized insulated unheated tube and rain cup of the larger pre-2013 design, which were subsequently replaced by a smaller improved design on 2 July 2014. We found that the larger intake tube and rain cup initially used, resulted in substantially under-estimated turbulent exchange and fluxes of H₂O relative to the LGR-FGGA-24EP with heated tubing (Figs. S1 and S2e). Therefore, only data collected after this change were used for the comparison (LI-7200/LGR-FGGA-24EP). The LI-7200-101 flow module was used to automatically regulate and maintain the flow rate at 15 l min⁻¹. The LGR-FGGA-24EP analyzer and associated dry-scroll vacuum pump, sampling air at a rate of 20 l min⁻¹ (N 940.5 APE-W, KNF Neuberger AG, BALTERSWIL, Switzerland) were housed inside water-proof, insulated boxes (Grizzly Coolers, Decorah, Iowa). To minimize condensation inside the inlet tube of the LGR-FGGA-24EP analyzer, the tubing (PFA Tubing, 3/8 in. OD × 0.062 in., Swagelok, Solon, Ohio) was wrapped in heating tape, and both the inlet tube and the heating tape were insulated. The inlet tubing was terminated with an inverted funnel and protected with flexible mosquito netting to prevent water intake, ice formation at the inlet of the tubing, and mosquitos from entering the sample line. A 2 μm stainless filter (SS-4FW-2 1/4T × 1/4T, Swagelok) was installed before the analyzer inlet to prevent sample cell contamination. For the cross-comparison of CO₂ and LE fluxes from the LI-7200 and LGR-FGGA-24EP analyzers at ATQ, we used three-dimensional wind speed from the CSAT3.

Table 1
Sensor configurations and distances between analyzers at each site. Heated intake tubes are indicated by subscript 'H'. The LGR-FGGA-24EP was manufactured by Los Gatos Research Inc., CA, USA; the LI-7500, LI-7200, and LI-7700 by LI-COR Biosciences Inc., NE, USA; the CSAT3 by Campbell Scientific Inc., UT, USA; the Gill WMP and R3 by Gill Instruments Ltd., Hampshire, UK; and the Metek uSonic-3 Class A by Metek GmbH, Elmshorn, DE.

Sonic anemometers					
Site	Model	Height (m)	Orientation (°)	Heating (dist. to Metek (m))	
CMDL	Gill WMP ^a	4.17	35	non-heated	
BES	CSAT3 ^a	2.18	60	non-heated	
ATQ	CSAT3 ^a	2.28	175	non-heated (0.35)	
	Gill R3	2.28	0	non-heated (0.56)	
	Metek	2.28	94	continuous	
IVO	Metek ^a	3.42	205	intermittent	
Gas analyzers					
Site	Model	Height (m)	Gas species	Tube length (m) (dist. to CP (m)) ^b	Dist. to primary anemometer (m)
CMDL	LGR-FGGA-24EP	4.18	CO ₂ /H ₂ O/CH ₄	5.71 _H	0.18
	LI-7700	4.12	CH ₄	(0.23)	0.23
BES	LI-7500	1.60	CO ₂ /H ₂ O	(0.37)	0.20
	LGR-FGGA-24EP	2.00	CO ₂ /H ₂ O/CH ₄	4.50 _H	0.17
ATQ	LI-7200	2.25	CO ₂ /H ₂ O	1.20 (0.07)	0.44
	LGR-FGGA-24EP	2.30	CO ₂ /H ₂ O/CH ₄	3.12 _H	0.43
IVO	LI-7200	3.22	CO ₂ /H ₂ O	1.20	0.14
	LI-7700	3.12	CH ₄	–	0.45

^a Primary anemometer used for flux calculation in gas analyzer comparisons.

^b Distance to the closed or (en)closed-path (CP) analyzer used in comparisons.

Raw signals were collected at 10 Hz using a CR3000 (Campbell Scientific, Logan, UT, USA).

At BES, the set-up for the LGR-FGGA-24EP was similar to that in ATQ. The open-path LI-7500 at BES was mounted at a 20° angle to minimize water build-up on the windows of the analyzer. Three-dimensional wind speed was measured with the CSAT3 anemometer and raw signals of each instrument were collected at 10 Hz using a CR3000.

At CMDL, the wind components from the Gill WindMaster Pro were used for flux calculations. Raw signals of the LI-7700 and WindMaster Pro were collected at 10 Hz using the LI-7550 Analyzer Interface Unit, while a CR3000 also recorded data from the LGR-FGGA-24EP and WindMaster Pro at 10 Hz. The automated LI7700 sensor mirror washer was activated based on signal strength of the analyzer to maximize data quality.

At IVO, wind components from the intermittently heated Metek uSonic-3 Class A anemometer were used for flux calculations with CO₂/H₂O data from an (en)closed-path LI-7200 and CH₄ from an open-path LI-7700. Raw 10 Hz signals were collected with the LI-7550 Analyzer Interface Unit. A 5-gallon jug was installed to supplement the washer fluid basin used with the automated LI-7700 sensor mirror washer, which was activated based on the signal strength of the analyzer.

2.5. Data quality control, processing, and analyses

The LGR-FGGA-24EP sensors were calibrated by the manufacturer just before being shipped to Alaska. The LI-7500 and LI-7200 analyzers were all calibrated at least twice per year in the laboratory in Barrow during 2013–2015. Half-hourly eddy covariance fluxes were calculated using EddyPro[®] (www.licor.com/eddypro). De-spiking and absolute limit determination were included in the preliminary processing of raw signals (Vickers and Mahrt, 1997) and outliers were discarded. Angle of attack errors were corrected according to Nakai et al. (2006) and Nakai and Shimoyama (2012), respectively for the Gill R3 and WindMaster Pro anemome-

ters. A double axis rotation of the wind vector was performed (Wilczak et al., 2001) and the block-averaging method was used to extract turbulent fluctuations from time series (Gash and Culf, 1996). Time lags between vertical wind speed and the variable of interest were determined for each averaging period by covariance maximization. Low frequency spectral corrections were applied according to the analytic method described in Moncrieff et al. (2004). High frequency spectral corrections were applied depending on the setup: the fully analytic method of Moncrieff et al. (1997) was adopted for the open-path systems (LI-7500, LI-7700), which includes a correction for sensor separation effects; an *in-situ* spectral correction method (Ibrom et al., 2007) was used for the closed-path analyzers (LI-7200, LGR-FGGA-24EP) as it is a more suitable method to describe attenuation along the intake tube walls. For the closed-path analyzers, a correction was also applied to account for sonic anemometer and analyzer separation according to Horst and Lenschow (2009).

For the open-path LI-7500 analyzer at BES, the WPL correction (Webb et al., 1980) and the self-heating correction adapted to Arctic conditions were also applied (Burba et al., 2008; Oechel et al., 2014). Mixing ratio data were used from closed-path analyzers (LI-7200) or data were converted to mixing ratios (LGR-FGGA-24EP), thus avoiding the need for WPL corrections. For the open-path LI-7700, a spectroscopic correction was computed with the WPL correction to account for the modification in the shape and width of the absorption line due to changes in temperature-pressure-water vapor (McDermitt et al., 2011). As a QA/QC test of the final fluxes, we used the standard flags (0–1–2) defined by Mauder and Foken (2006) and data with a flag = 2 were discarded. Remaining flux data were filtered for insufficient atmospheric turbulence (Reichstein et al., 2005) with a friction velocity threshold of 0.1 m s⁻¹. Remaining spikes were removed using a 30-day moving window that advanced one day at a time and any half-hours that exceeded ±2 standard deviations from the mean for that half-hour were discarded.

In ATQ, the anemometer flux comparisons were limited to the wind sector between the roughly perpendicularly oriented

CSAT3 and Metek (Table 1) to minimize flow distortion effects. We performed orthogonal regression analyses, as there was no true dependent variable or a control, and we therefore needed to account for errors in both flux estimates. Since R^2 values cannot be obtained from orthogonal regression, we have reported Pearson's correlation coefficient (r) associated with each comparison. In addition to the 1:1 regression comparisons, we analyzed the differences between flux measurement pairs by plotting the distribution of differences (Δ flux values) and fitting Laplace (double exponential) probability density functions to obtain the mean difference (bias) and spread (variance) of differences for each comparison.

To compare annual estimates of CO_2 derived from various sensor combinations, we filled gaps in the half-hourly fluxes using the online eddy covariance gap-filling tool (<http://www.bgc-jena.mpg.de/~MDIwork/eddyproc>) which employs standard methods of Reichstein et al. (2005). Methane fluxes were gap-filled using an artificial neural network (ANN) (Dengel et al., 2009; Zona et al., 2016). Meteorological inputs to the ANN included air temperature, soil temperature at 10 cm depth, photosynthetic photon flux density (PPFD), vapor pressure deficit (VPD), and two sonic cross wind components, (u and v). The ANN was run 25 times and the median value was used to fill gaps in half-hourly flux time series.

To assess the uncertainty associated with each annual sum, we applied the 'paired days' approach to estimate random uncertainty of measured fluxes (Hollinger and Richardson, 2005). We used a Monte Carlo simulation to sample randomly from double-exponential distributions defined by the sigma values that resulted from the paired-days analysis (Dragoni et al., 2007). The median half-hourly uncertainty from 250 simulations was used in the annual assessment. The uncertainty associated with the gap-filling approach was assessed by simulating gaps and comparing synthetic data to observations (Reichstein et al., 2005), and half-hourly uncertainties were propagated in quadrature (Taylor, 1997) to obtain annual values. All data analyses were performed with Matlab (R2014a, MathWorks, Natick, MA, USA).

3. Results

3.1. Sonic anemometer comparisons

The half-hourly sensible heat fluxes (H) calculated with the unheated anemometers (CSAT3 and Gill R3) revealed a good comparison, with a slope of 1.01 and Pearson's r of 0.96 (Fig. 1a). The sensible heat fluxes derived from the continuously heated Metek were higher on average than the (unheated) CSAT3, with a slope of 1.12 and intercept of 7.27 W m^{-2} (Fig. 1b). Further comparison between these two sonic anemometers, revealed that differences in the variance in sonic temperature (T_s) were negligible (Fig. 2a), whereas there was higher variance in the vertical wind component (w) measured by the heated Metek than the CSAT3 (red line; slope = 1.17 and intercept = $-0.01 \text{ m}^2 \text{ s}^{-2}$) (Fig. 2b).

We explored the effect of heating the Metek at ATQ and potential influence of over-estimated fluctuations in w on the gas fluxes by comparing F_{CO_2} , LE, and F_{CH_4} derived from both the CSAT3 and the heated Metek, paired with the LGR-FGGA-24EP closed-path gas analyzer. We found that the heated Metek resulted in higher LE than the unheated CSAT3-derived fluxes, with a slope of 1.19 (Fig. 3a) and a mean bias (Δ LE) of -3.77 W m^{-2} (Fig. 4a). Discrepancies in CO_2 and CH_4 fluxes from the two sensor pairs were smaller, with slopes of 1.09 and 1.07 in the regressions, respectively (Fig. 3c and e), and delta flux values were also small for F_{CO_2} ($-0.03 \mu\text{mol m}^{-2} \text{ s}^{-1}$) and F_{CH_4} ($-0.05 \text{ mgC m}^{-2} \text{ h}^{-1}$) (Fig. 4c and e). Given this smaller offset in the direct comparison of C fluxes, the annual sums of F_{CO_2} from these two sensor pairs were also very similar (within 5%). Specifically, from 1 October 2013

to 30 September 2014 at ATQ, the heated Metek – LGR sensor pair resulted in an estimated loss of $7.5 \pm 1.4 \text{ gC-CO}_2 \text{ m}^{-2} \text{ yr}^{-1}$ and the CSAT3 – LGR sensor pair resulted in an estimated loss of $7.9 \pm 1.3 \text{ gC-CO}_2 \text{ m}^{-2} \text{ yr}^{-1}$ (Table 2). This small difference in annual F_{CO_2} resulted from the compensating effect of slightly higher uptake during the day and slightly higher losses at night estimated from the Metek-derived fluxes, a consequence of the higher variance in the vertical wind component (w). For example, winter CO_2 losses were 9.2% higher and summer uptake was 6.7% higher when estimated from the Metek – LGR sensor pair (Fig. 5a). Additionally, when isolating data from June, July and August 2014, the mean daytime CO_2 uptake and mean night time CO_2 losses were also approximately $0.1 \mu\text{mol m}^{-2} \text{ s}^{-1}$ larger from the Metek – LGR pair.

The annual F_{CH_4} at ATQ from the heated Metek and unheated CSAT3 were identical ($3.7 \text{ gC m}^{-2} \text{ yr}^{-1}$) (Table 2). Furthermore, there was very little temporal shift in the F_{CH_4} cumulative time series from these two sensor pairs (Fig. 5b). Therefore, timing and seasonal comparisons are also constrained for F_{CH_4} between the heated and unheated setup.

To separate the impact of heating from the potential differences in the performance of the Metek and CSAT3, we de-activated heating of the Metek from 17 March 2015 to the present day. Using the same QA/QC protocol, we found better agreement in H , whereby the regression slope was reduced to 1.06 (Fig. 1b), suggesting the continuous heating was responsible for at least half of the over-estimation of $\sigma^2 w$ (Fig. 2b), in addition to reducing heating-related errors. However, over-estimation of LE persisted even after the heating of the Metek was deactivated (slope = 1.20, Fig. 3b), with only a slight improvement in the mean bias to -3.21 W m^{-2} (Fig. 4b). Finally, the comparison of F_{CO_2} and F_{CH_4} between the heated and unheated setup remained very good (slopes of 1.06 and 0.99, respectively) (Fig. 3d and f). The mean bias for F_{CO_2} dropped to 0, while that for F_{CH_4} was reduced to $-0.01 \text{ mgC m}^{-2} \text{ h}^{-1}$ (Fig. 4d and f).

The intermittent heating system for the Metek at IVO successfully de-iced the transducers during cold periods (Fig. 6), bypassing the observed biases to the fluxes. The very noisy flux data associated with ice build-up was minimized during the short periods when heating was activated, and the post-heating sensible heat fluxes were comparable to pre-heating values (Fig. 6), suggesting only a temporary influence, and no long-term biases on the fluxes. Despite losing 3.2% of data from the Metek at IVO during heating activation (which we removed during post-processing), the annual data coverage of H from that site was the same as that of the continuously heated Metek at ATQ (64%) and the winter data coverage was similar (50% and 46% for IVO and ATQ, respectively) (Table 3). However, it should be noted that due to unrelated technical issues at ATQ that led to data losses during winter, the available data before QA/QC and filtering was lower at that site than IVO (Table 3).

3.2. Gas analyzer comparisons

3.2.1. Closed-path and (en)closed-path CO_2 and H_2O analyser comparison

We compared fluxes from the closed-path LGR-FGGA-24EP and the (en)closed-path LI-7200 at ATQ using the CSAT3 anemometer. F_{CO_2} was very similar between the two sensor pairs with a slope of 0.99 and -0.01 intercept ($r = 0.87$, $P < 0.001$) (Fig. 7a). The ΔF_{CO_2} distribution also suggested very low bias ($\mu = 0.01 \mu\text{mol m}^{-2} \text{ s}^{-1}$) with generally tight spread ($\sigma = 0.53 \mu\text{mol m}^{-2} \text{ s}^{-1}$) (Fig. 8a). The resulting annual total CO_2 fluxes derived from the two sensor pairs were within $1.4 \text{ gC m}^{-2} \text{ yr}^{-1}$, with the LI-7200 resulting in slightly larger CO_2 loss ($9.3 \pm 1.1 \text{ gC m}^{-2} \text{ yr}^{-1}$) than the LGR-FGGA-24EP ($7.9 \pm 1.3 \text{ gC m}^{-2} \text{ yr}^{-1}$) (Table 2). Primary differences in the cumulative CO_2 flux trajectories were slightly higher respiratory losses of late autumn CO_2 from the LGR-FGGA-24EP with subse-

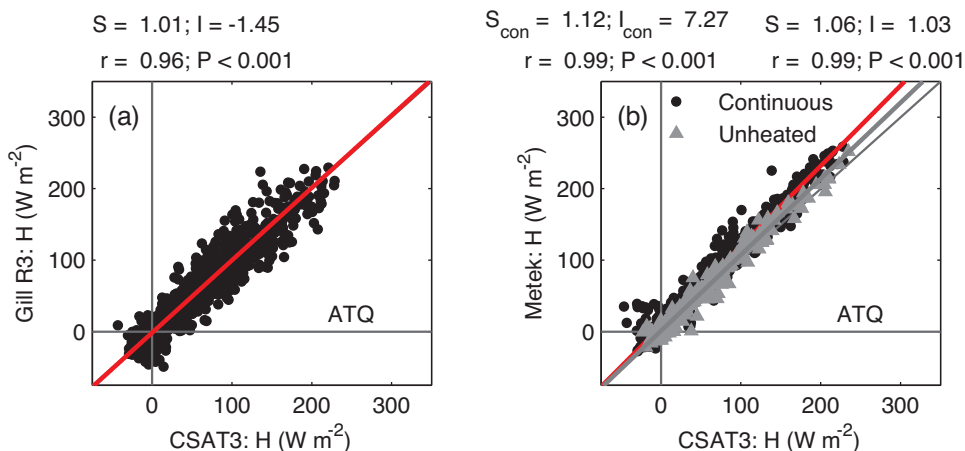


Fig. 1. Comparisons of half-hourly sensible heat fluxes (H) at ATQ derived from the (unheated) CSAT3 anemometer and the (unheated) Gill R3 ($n=634$) (a) and the heated Metek ($n=634$) (b) from 1 October 2013 to 30 September 2014. The red line in panel b corresponds to the heated Metek data while the grey line and symbols represent data after heating of the Metek at ATQ was fully de-activated from 17 March to 11 June 2015 ($n=581$). Regression coefficients with the 'con' subscript indicates results from the continuously heated Metek data. In this and all of the following regression figures, 'I' denotes the fitted intercept in units given on the x and y-axes, and 'S' denotes the slope of the regression. (For interpretation of the references to color in this figure legend, the reader is referred to the web version of this article.)

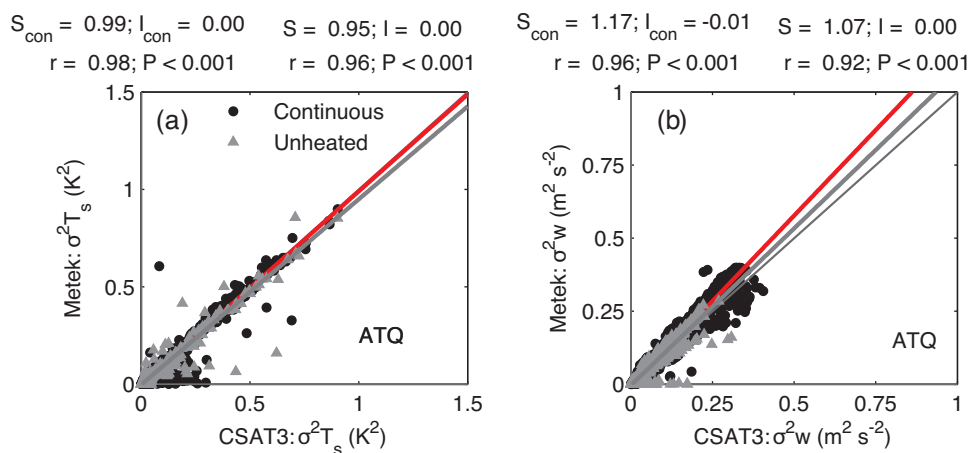


Fig. 2. Comparisons of the CSAT3 and the heated Metek at ATQ of half-hourly variance in T_s ($n=634$) (a) and w ($n=554$) (b) from 1 October 2013 to 30 September 2014. The red line in panel b corresponds to the heated Metek data while the grey line and symbols represent data collected after heating of the Metek at ATQ was fully de-activated from 17 March to 11 June 2015 ($n=543$). Regression coefficients with the 'con' subscript represent results from the continuously heated Metek data. (For interpretation of the references to color in this figure legend, the reader is referred to the web version of this article.)

Table 2

Annual total F_{CO_2} and F_{CH_4} estimated with different sensor combinations at ATQ, BES, and CMDL. See Section 2.5 for a description of the uncertainty estimation.

Site	Gas analyzer	Anemometer	Annual NEE [gCm ⁻² yr ⁻¹]	Annual F_{CH_4} [gCm ⁻² yr ⁻¹]
ATQ	LGR	CSAT	7.9 (±1.3)	3.7 (±0.28)
	LGR	Metek (heated)	7.5 (±1.4)	3.7 (±0.26)
	LI-7200	CSAT	9.3 (±1.1)	-
BES ^a	LGR	CSAT	-14.2 (±1.7)	-
	LI-7500	CSAT	-17.0 (±1.1)	-
CMDL	LGR	Gill WMP	-	4.9 (±0.27)
	LI-7700	Gill WMP	-	4.5 (±0.31)

^a Flux integrals for BES were calculated for 1 May to 31 October.

quent greater spring CO_2 uptake (Fig. 5a). Latent heat fluxes at ATQ from the LI-7200 were generally somewhat higher than from the LGR-FGGA-24EP with a slope of 0.86 from the regression ($r=0.98$, $P<0.001$) (Fig. 7c). This was also reflected in the mean bias in ΔLE of 3.22 W m^{-2} , with tight spread ($\sigma = 7.60 \text{ W m}^{-2}$) (Fig. 8c).

3.2.2. Open-path and closed-path CO_2 and CH_4 analyser comparison

We used data from BES to compare F_{CO_2} derived from the closed-path LGR-FGGA-24-EP and the open-path LI-7500, both paired with the CSAT3 anemometer. There were less available data from the LI-7500 and more noise in fluxes from both sensor pairs at BES than was observed at ATQ, and thus the amount

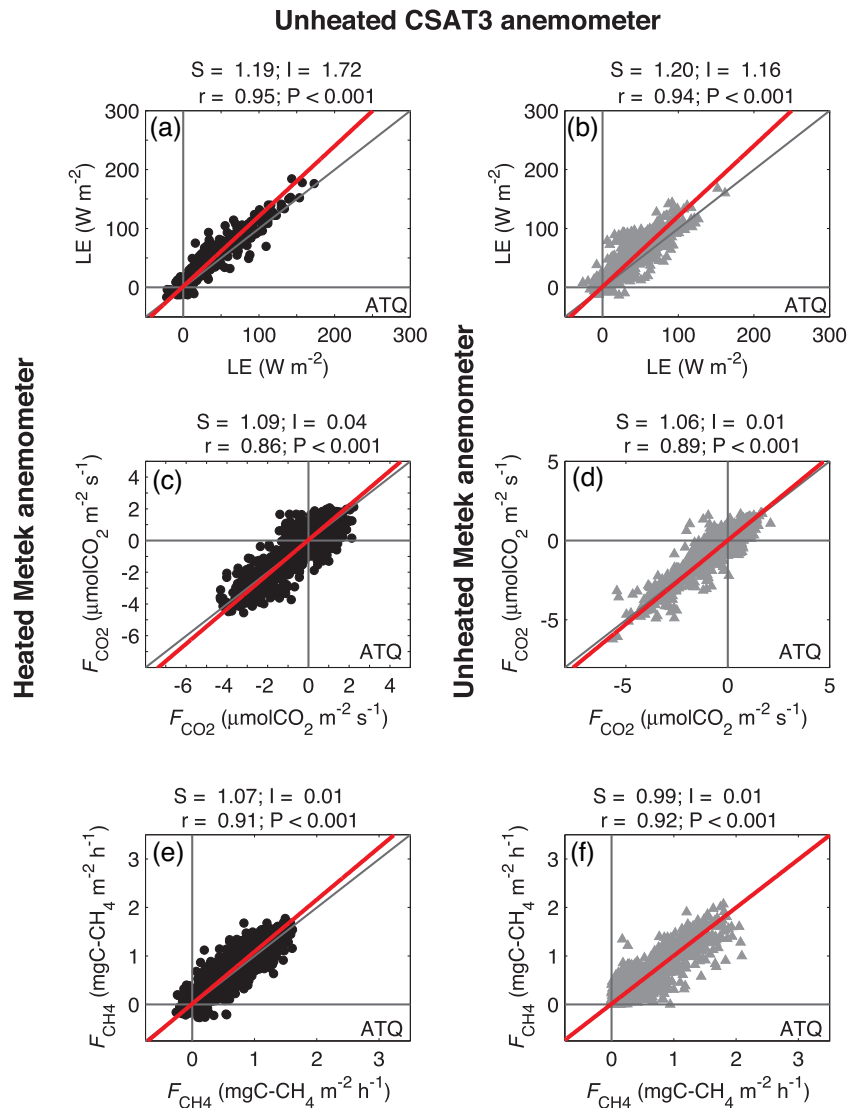


Fig. 3. Comparison of 30-min average LE ($n = 2316$) (a), F_{CO_2} ($n = 2167$) (b), and F_{CH_4} ($n = 3563$) (c) fluxes derived from the heated Metek sonic anemometer (y-axis) and the unheated CSAT3 anemometer, and LE ($n = 2969$) (b), F_{CO_2} ($n = 2689$) (d), and F_{CH_4} ($n = 2058$) (f) from the unheated Metek and unheated CSAT3, in all cases paired with the LGR closed-path analyzer at ATQ from 1 October 2013 to 22 July 2015.

of data used in these comparisons was smaller (Table 3). As a result, the regression comparison showed considerable scatter with a slope of 1.28 and $0.29 \mu\text{mol m}^{-2} \text{s}^{-1}$ intercept ($r = 0.61$, $P < 0.001$) (Fig. 7b). Despite the high degree of spread in the distribution of ΔF_{CO_2} ($\sigma = 1.13 \mu\text{mol m}^{-2} \text{s}^{-1}$), the mean bias was low ($\mu = -0.04 \mu\text{mol m}^{-2} \text{s}^{-1}$) (Fig. 8b).

Ice and snow build-up on the windows of the open-path LI-7500, for which no winterization was attempted during 2013–2015, led to particularly poor data coverage during cold periods at BES and as little as 10% of CO_2 flux data remained after quality control filtering for the period from 1 October 2013 to 23 April 2014 (i.e. winter). We therefore estimated integral CO_2 fluxes only for late spring and summer (1 May to 31 October 2015) at BES. Total flux calculated for this period from the LGR-FGGA-24EP was $-14.2 \pm 1.7 \text{ gC m}^{-2} \text{ summer}^{-1}$ and from the LI-7500 was $-17.0 \pm 1.1 \text{ gC m}^{-2} \text{ summer}^{-1}$, with most of this difference derived from slightly larger spring thaw-out CO_2 losses and summer uptake measured by the LI-7500 (Fig. 5c). Generally, despite potentially large differences in instantaneous measurements between these two set-ups, and larger spectral corrections required for LGR-FGGA-

24EP flux calculations (Table 4), mean flux values from longer periods (seasonal) converge to values within uncertainty ranges.

Methane fluxes were compared at CMDL using the LGR-FGGA-24EP closed-path analyser and the LI-7700 open-path sensor. The regression comparison resulted in a slope of 0.86 with an intercept of $0.05 \text{ mgC m}^{-2} \text{ h}^{-1}$ ($r = 0.68$, $P < 0.001$) (Fig. 7d). The $0.02 \text{ mgC m}^{-2} \text{ h}^{-1}$ mean ΔF_{CH_4} suggested a very small bias toward higher fluxes derived from the open-path LI-7700 (Fig. 8d). However, the data coverage in CMDL was markedly better from the LGR-FGGA-24EP with 54% coverage over the entire measurement year, whereas coverage was 26% for the open-path LI-7700 (Table 3). As expected, the seasonality in flux data coverage from these two sensors showed much higher cold-season data capture rates with the closed-path LGR-FGGA-24EP. Using the seasonal breakdown based on PPFD and temperature described in Oechel et al. (2014), we found the LGR-FGGA-24EP data coverage was 40, 58, 81, and 65% for winter, spring, summer, and fall, respectively. Whereas the data capture rates from the LI-7700 at CMDL during those seasons were 14, 46, 49, and 27%, respectively. On the other hand, at IVO the annual data coverage obtained by the open-path LI-7700 paired with the intermittently heated Metek anemometer

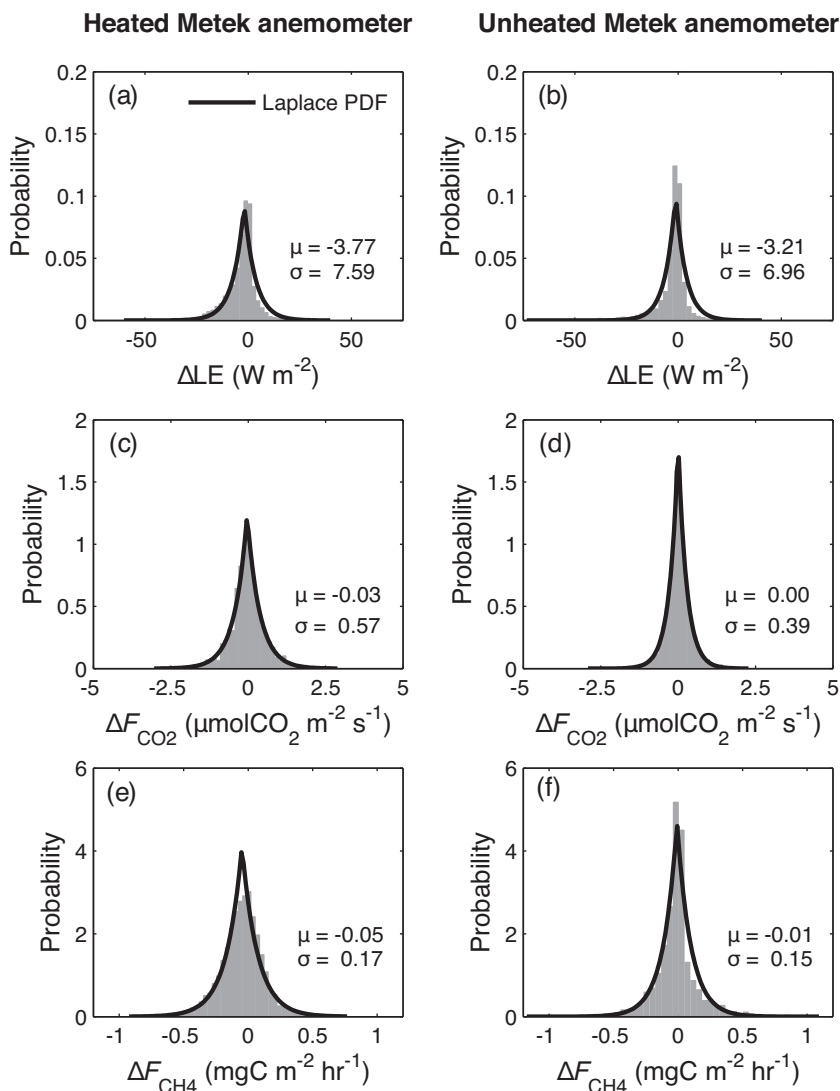


Fig. 4. Distributions of flux differences (Δ flux) from the analyzer pairs being compared in Fig. 3. Delta values were calculated as CSAT3 LE – Metek LE (a, b), CSAT3 F_{CO_2} – Metek F_{CO_2} (c, d), and CSAT3 F_{CH_4} – Metek F_{CH_4} (e, f). Distributions were fitted with Laplace (double exponential) maximum likelihood $ML = \frac{1}{2}\beta e^{-|x-\mu|/\beta}$, where $\sigma = \sqrt{2}\beta$.

Table 3
Data coverage for fluxes calculated with each sensor configuration. The continuously heated Metek is indicated by (con), the intermittently heated Metek is indicated by (int), closed- and (en)closed-path gas analyzers are indicated by (CP), and open-path analyzers are indicated by (OP). The available data column excludes only those for which a flux could not be calculated due to loss of power (<5% for all sites), instrument malfunction, and active rain or heavy fog, which causes high frequency data to be out of range.

Site	Flux	Sensor (pair)	Available data (%)	Annual coverage following QA/QC, spike removal (%)	Winter coverage (%)
ATQ	H	CSAT	66	52	31
	H	Metek (con)	76	64	46
	H	Gill R3	64	47	25
IVO	H	Metek (int)	91	64	50
BES	F_{CO_2}	LI-7500 (OP) – CSAT	51	30	10
	F_{CO_2}	LGR (CP) – CSAT	88	70	41
ATQ	F_{CO_2}	LI-7200 (CP) – CSAT	66	48	27
	F_{CO_2}	LGR (CP) – CSAT	53	53	32
	F_{CO_2}	LGR (CP) – MTK (con)	76	61	46
ATQ	LE	LI-7200 (CP) – CSAT	66	46	26
	LE	LGR (CP) – CSAT	66	52	35
	LE	LGR (CP) – MTK (con)	76	67	46
ATQ	F_{CH_4}	LGR (CP) – CSAT	66	52	31
	F_{CH_4}	LGR (CP) – MTK (con)	76	61	44
BRW	F_{CH_4}	LI-7700 (OP) – Gill WP	27	26	14
	F_{CH_4}	LGR (CP) – Gill WP	55	54	40
IVO	F_{CH_4}	LI-7700 (OP) – Metek (int)	65	47	35

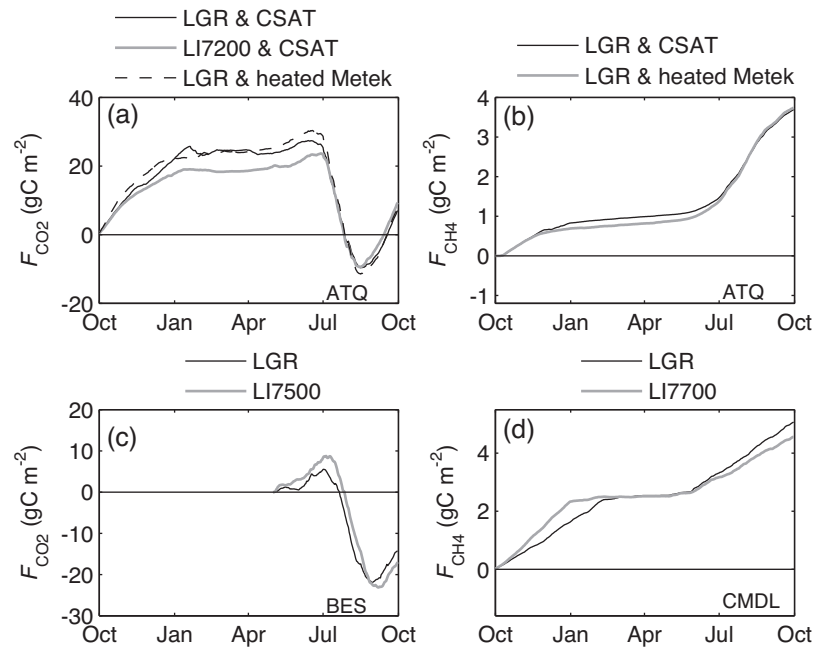


Fig. 5. Cumulative CO_2 from the open and closed-path analyzers in BES paired with the CSAT3 (Table 2) (a), F_{CO_2} from the closed and (en)closed-path analyzers and heated and unheated anemometers in ATQ (c). Cumulative CH_4 fluxes from the open and closed-path analyzers in CMDL (b), and from the heated and non-heated anemometers in ATQ (d).

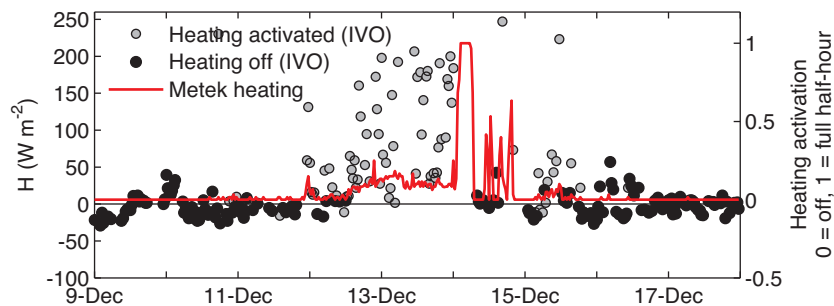


Fig. 6. Sensible heat fluxes from IVO during a heating activation of the intermittently heated Metek anemometer. The solid red line shows the duration of heating as 30-min average values of the heating flag, which was set to 0 (off) or 1 (on) depending on the activation status. Grey points show noisy data resulting from the build-up of ice and snow and the resulting activation of anemometer heating. (For interpretation of the references to color in this figure legend, the reader is referred to the web version of this article.)

was 47% and winter coverage was 35% (Table 3), indicating that good coverage is possible with open-path CH_4 analysers farther inland from the coast, with lower humidity (annual average RH of 75% and 87% at IVO and CMDL, respectively) and less influence of salt spray. Furthermore, despite the small bias in the fluxes at CMDL toward higher LI-7700 F_{CH_4} , and lower data coverage during cold periods, the annual sums from the open and closed-path set-ups were not significantly different (Table 2), with only slight deviations in the cumulative trajectory in winter and autumn (Fig. 5d).

4. Discussion

4.1. Sonic anemometer comparisons

Continuous heating of the Metek sonic anemometer at ATQ considerably increased the data coverage, especially in winter, relative to the unheated CSAT3 and Gill R3 anemometers (Table 3). However sensible heat and gas fluxes were over-estimated with the heated Metek. Recently, Frank et al. (2013) suggested that non-orthogonal sonic anemometers may under-estimate the vertical wind component and H , which was also found by Mauder et al. (2007) for two non-orthogonal designs. However, Loescher et al.

(2005) found higher H from the CSAT3 compared to orthogonal anemometers. All of the anemometers compared in this study were non-orthogonal, however our results suggest that the anemometer geometry (horizontal head vs. vertical head) had a relatively small impact, on wind components and sensible heat and C fluxes at ATQ. The anemometer heating had the most important influence on comparisons. A similar result was reported from the BOREAS IV campaign, where several heated anemometers, including an earlier Metek model (USA-1 55W), were compared to unheated anemometers (including a Gill R3) and a heightened sensitivity to the vertical wind component was noted in the heated models (Tammelin et al., 1998). Nonetheless, the observed over-estimation of vertical wind variations by the heated Metek in this study led only to a relatively small increase in F_{CO_2} (both uptake and losses) and F_{CH_4} (Fig. 3c and e). As a result, there was a small difference in the estimated annual CO_2 fluxes compared to the CSAT-derived fluxes, and the two estimates had overlapping uncertainties (Table 2). This result suggests that despite a small over-estimation of C gas fluxes derived from a continuously heated anemometer, the increase in data coverage can still lead to defensible annual estimates.

Despite improved data coverage and relatively small effects on long-term fluxes observed at ATQ, continuous heating may not

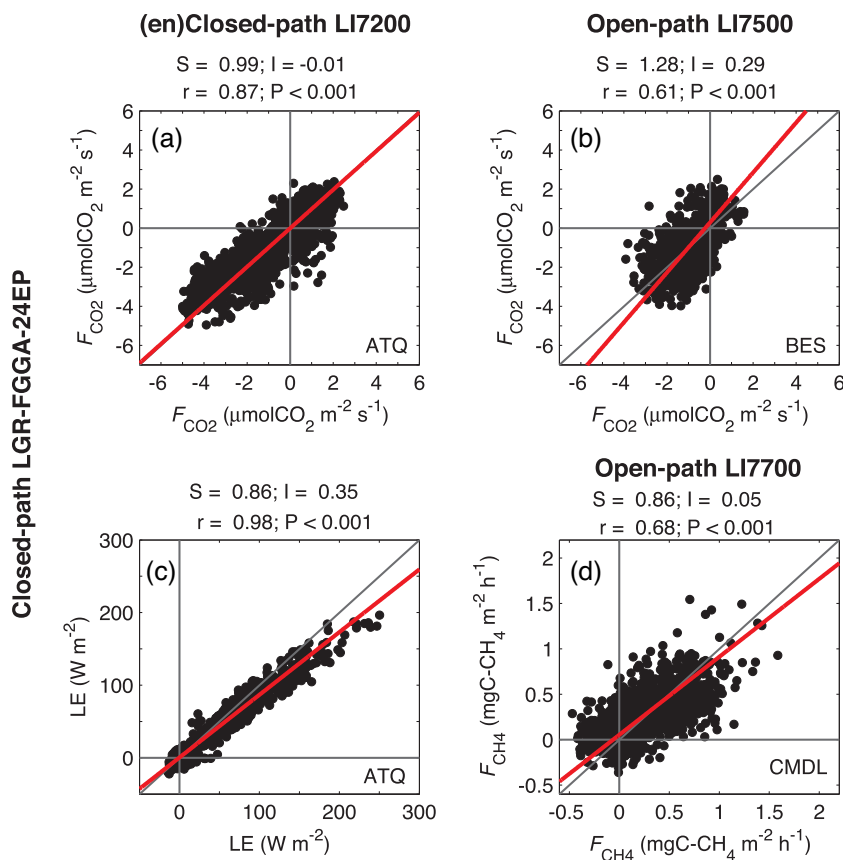


Fig. 7. Comparisons of 30-min average F_{CO_2} ($n = 5036$) (a) and LE ($n = 2837$) (c) between closed and (en)closed-path sensors ATQ, and comparisons of F_{CO_2} ($n = 790$) (b) and F_{CH_4} ($n = 1681$) (d) between open and closed-paths sensors at BES and CMDL, respectively.

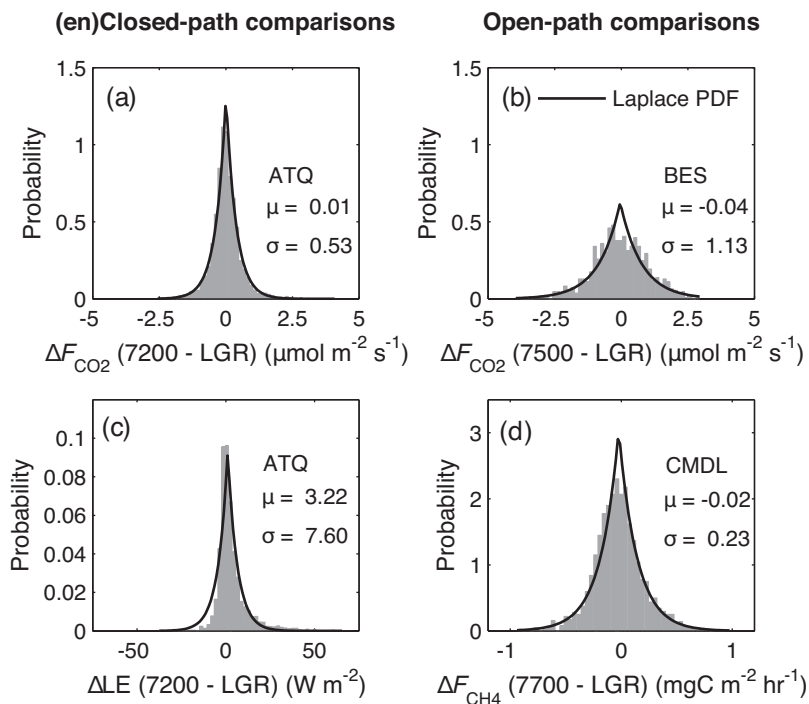


Fig. 8. Distributions of flux differences ($\Delta flux$) from the analyzer pairs being compared in Fig. 6. Delta values were calculated as (en)closed-path – closed-path fluxes (b, a and c) and open-path – closed path fluxes (b and d).

be the optimal choice, particularly for remote flux towers where power consumption is critical for site operation. An intermittent heating approach, such as that devised in this study, provides a better alternative. This minimizes power consumption, reduces heating-related errors in fluxes, and retains very similar data coverage compared to continuously heated systems (Figs. 2 and S3; Table 3). We recommend that intermittent heating be implemented in all sites operating in cold climates, to increase data coverage during the cold season and avoid overestimating fluxes in all periods.

4.2. Gas analyzer comparisons

We found that despite the potential for relatively large instantaneous differences in fluxes as well as the larger spectral corrections required for longer-tube LGR-FGGA-24EP fluxes due to sensor time response, tubing and filter attenuation, and intake assembly, the resulting annual CO₂ fluxes did not differ significantly from the shorter-tube LI-7200. Burns et al. (2014) also found good comparisons between the LI-7200 and an older model LI-6262 close-path analyzer with a longer intake tube after data treatment and post-processing were properly accounted for, despite differing spectral response. These results provide a measure of confidence in carbon flux estimates obtained by closed-path gas analyzers of various designs when upgrading long-term sites or planning new experiments, provided that careful spectral corrections are applied to each design using data-driven, *in-situ* methods. On the other hand, latent heat fluxes from the LGR-FGGA-24EP with heated tube in this study were slightly under-estimated compared to the LI-7200 with a shorter, unheated tube (ATQ) (Figs. 7 c and 8 c). The longer tube length (3.12 m compared to 1.2 m) of the LGR-FGGA-24EP (Table 1) at ATQ likely contributed to more attenuation of the H₂O signal compared to the LI-7200, leading to spectral correction factors that did not fully compensate for this signal loss (Table 3, Fig. S2). This was noted in other comparisons (Burns et al., 2014), and the attenuation of H₂O signals due to intake tubing remains a trade-off in eddy covariance systems where increased data coverage is desired (Lenschow and Raupach, 1991; Leuning and Judd, 1996). At the wettest site, BES, H₂O signal attenuation was so severe that spectral correction factors of 300–400% applied to the closed-path LGR-FGGA-24EP LE fluxes (Table 3) were insufficient to calculate comparable direct comparisons with the LI-7500 (not shown). Other studies have found similar under-estimation of LE from closed-path systems relative to open-path (Haslwanter et al., 2009; Ueyama et al., 2012). The BES site exhibits more extensive inundated areas relative to the other study sites (Zona et al., 2009; Zona et al., 2016), and the attenuation of H₂O signals can be strongly influenced by relative humidity (Runkle et al., 2012), especially if the heating of the intake tube is not uniform (Mammarella et al., 2009). Reductions in intake tube lengths and funnel sizes as well as improvements to the tube heating system should be investigated in order to improve H₂O flux measurements in future work at these cold, inundated sites.

Fluxes of CO₂ from the open and closed-path systems at BES compared well after applying differing spectral correction factors (Table 4), while more noise in the fluxes was observed at this site leading to a large spread in ΔF_{CO_2} . A primary concern between sensor configurations for CO₂ fluxes at BES was data coverage during cold periods. The lack of reliable CO₂ flux data from the non-winterized open-path analyzer for a large part of the winter precluded the estimation of a full annual CO₂ budget at this site. Despite this, comparable flux integrals were obtained during warmer seasons and estimates from the different sensor combinations had overlapping uncertainties. Oechel et al. (2014) noted the difficulty in maintaining open-path analyzers during the Arctic winter and found that data capture rates fell below 15% during this period. This was, in part, due to the inability to safely access

Table 4

Comparison of summary statistics associated with spectral correction factors applied to fluxes at each site with different gas analyzers.

Site	Flux & sensor	Spectral correction factors		
		Median	1st quartile	3rd quartile
BES	F_{CO_2} LI-7500	1.14	1.13	1.16
	F_{CO_2} LGR	1.29	1.23	1.35
ATQ	F_{CO_2} LI-7200	1.15	1.11	1.20
	F_{CO_2} LGR	1.34	1.25	1.47
BES	LE LI-7500	1.14	1.13	1.15
	LE LGR	3.33	2.63	3.99
ATQ	LE LI-7200	2.34	1.99	2.89
	LE LGR	2.07	1.78	2.48
CMDL	F_{CH_4} LI-7700	1.15	1.13	1.17
	F_{CH_4} LGR	1.49	1.38	1.65

and maintain instrumentation at the tower, which is especially necessary for open-path sensors to keep the windows clean and unobstructed by snow and ice.

The open and closed-path F_{CH_4} compared well at CMDL (Figs. 5 d and 7 d). A number of eddy covariance CH₄ sensors have also successfully measured comparable fluxes (Detto et al., 2011; Peltola et al., 2013; Iwata et al., 2014). Therefore the choice of sensor may be adapted to the specific conditions and requirements (e.g. power availability) at a site if the research focus is on C–CH₄ gas fluxes and budgets. However, with increasing evidence for the importance of cold season emissions in the Arctic (Mastepanov et al., 2008; Mastepanov et al., 2013; Sturtevant et al., 2012; Zona et al., 2016), the most reliable data coverage during such periods currently requires closed-path analyzers, although heavily winterized open-path analyzers were not examined in this study. Coastal areas are particularly problematic in this regard given the higher humidity and the salt spray that affect the mirrors of open-path analyzers, leading to substantially higher data losses than areas farther inland, even when automated mirror cleaning is employed. For the inland sites, where low power availability prevents the use of close path CH₄ analyzers, we have found in this, and other studies (Zona et al., 2016), that the open path LI-7700 was able to successfully measure fluxes year-round with reasonable data coverage.

5. Conclusions

Using different eddy covariance sensor combinations on the same towers, we have shown that seasonal and annual CO₂ and CH₄ fluxes estimated using different gas analyzers and from heated and non-heated anemometers were within uncertainties. The remote locations and harsh winter conditions in the Arctic often necessitate the use of different site-specific instrumentation at each site. However, this does not preclude the ability to obtain comparable C fluxes if instruments are properly setup and fluxes are carefully processed. Heating sonic anemometers intermittently for de-icing, and excluding minimal data during the heating (~3% of the total data set), is the optimal solution for minimizing biases in wind components while maximizing data coverage (e.g. obtaining similar data coverage to a continuously heated anemometer). If sufficient power is available at the site, closed-path and (en)closed-path gas analyzers should be used to provide better data coverage than non-winterized open-path analyzers, especially in cold and wet environments, where 90% of data can be lost.

Acknowledgements

This work was funded by the Division of Polar Programs of the National Science Foundation (NSF) (Award 1204263); Carbon

in Arctic Reservoirs Vulnerability Experiment (CARVE), an Earth Ventures (EV-1) investigation, under contract with the National Aeronautics and Space Administration (NASA); and Department of Energy (DOE) Grant DE-SC005160. Logistical support was funded by the NSF Division of Polar Programs. The co-authors are also grateful to the United States Permafrost Association Early Career Grant for their financial support on field trips. This research was conducted on land owned by the Ukpeagvik Inupiat Corporation (UIC). We would like to thank the Global Change Research Group at San Diego State University, UMIAQ, UIC, CPS for logistical support, and Salvatore Losacco, Owen Hayman, and Herbert Njuabe for the help with the field data collection.

Appendix A. Supplementary data

Supplementary data associated with this article can be found, in the online version, at <http://dx.doi.org/10.1016/j.agrformet.2016.07.008>.

References

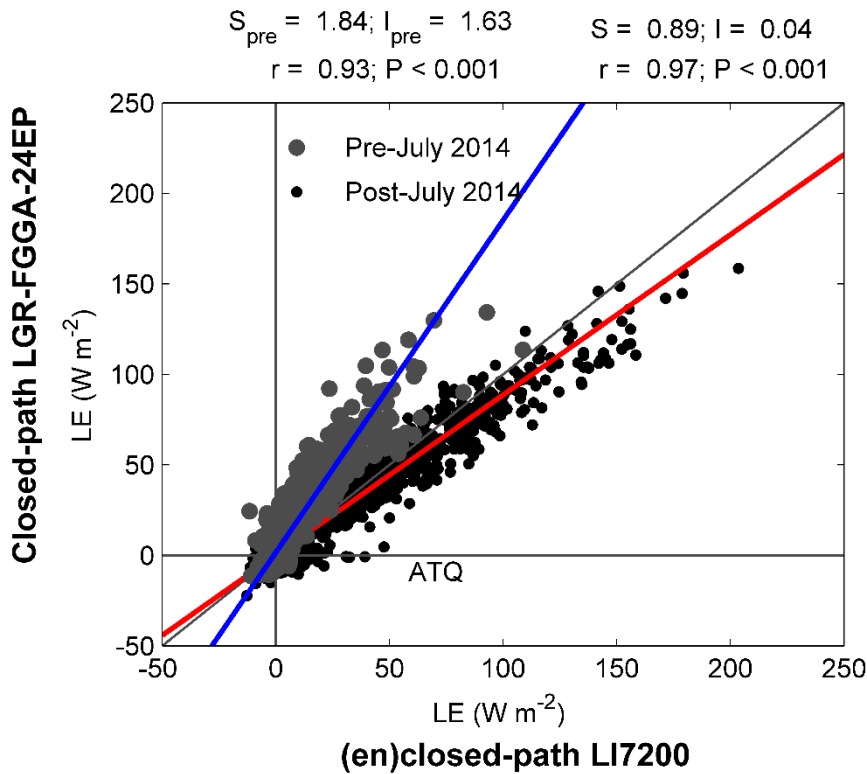
- Brown, J., Everett, K.R., Webber, P.J., MacLean Jr, S.F., Murray, D.F., et al., 1980. *An Arctic Ecosystem: The Coastal Tundra at Barrow, Alaska*. In: Brown, J. (Ed.), *Dowden, Hutchinson and Ross, Stroudsburg, PA*, pp. 1–29.
- Burba, G.G., McDermitt, D.K., Grelle, A., Anderson, D.J., Xu, L., 2008. Addressing the influence of instrument surface heat exchange on the measurements of CO₂ flux from open-path gas analyzers. *Global Change Biol.* 14, 1–23.
- Burba, G.G., McDermitt, D.K., Anderson, D.J., Furtaw, M.D., Eckles, R.D., 2010. Novel design of an enclosed CO₂/H₂O gas analyser for eddy covariance flux measurements. *Tellus B* 62 (5), 743–748.
- Burba, G.G., Schmidt, A., Scott, R.L., et al., 2012. Calculating CO₂ and H₂O eddy covariance fluxes from an enclosed gas analyzer using an instantaneous mixing ratio. *Global Change Biol.* 18, 385–399.
- Burba, G.G., 2013. *Eddy Covariance Method for Scientific, Industrial, Agricultural and Regulatory Applications: a Field Book on Measuring Ecosystem Gas Exchange and Areal Emission Rates*. LI-COR Biosciences, Lincoln, USA.
- Burns, S., Metzger, S., Blanken, P., et al., 2014. A comparison of infrared gas analyzers above a subalpine forest in complex terrain American Meteorological Society Committee on Atmospheric Measurements. In: *21st Conference on Applied Climatology/17th Symposium on Meteorological Observation and Instrumentation*, Westminster, Colorado, 9–13 June, p. 21.
- Detto, M., Verfaillie, J., Anderson, F., Xu, L., Baldocchi, D., 2011. Comparing laser-based open- and closed-path gas analyzers to measure methane fluxes using the eddy covariance method. *Agric. Forest Meteorol.* 151, 1312–1324.
- Dengel, S., Zona, D., Sachs, T., Aurela, M., Jammert, M., Parmentier, F.J.W., Oechel, W., Vesala, T., 2009. Testing the applicability of neural networks as a gap-filling method using CH₄ flux data from high latitude wetlands. *Biogeosciences* 10 (12), 8185–8200.
- Dragoni, D., Schmid, H.P., Grimmond, C.S.B., Loescher, H.W., 2007. Uncertainty of annual net ecosystem productivity estimated using eddy covariance flux measurements. *J. Geophys. Res.-Atmos.* 112 (D17), <http://dx.doi.org/10.1029/2006jd008149>.
- El-Madany, T.S., Griessbaum, F., Fratini, G., Juang, J.Y., Chang, S.C., Klemm, O., 2013. Comparison of sonic anemometer performance under foggy conditions. *Agric. Forest Meteorol.* 173, 63–73.
- Emmerton, C.A., St. Louis, V.L., Humphreys, E.R., Gamon, J.A., Barker, J.D., Pastorello, G.Z., 2015. Net ecosystem exchange of CO₂ with rapidly changing high Arctic landscapes. *Global Change Biol.*, <http://dx.doi.org/10.1111/gcb.13064>.
- Euskirchen, E.S., Bret-Harte, M.S., Scott, G.J., Edgar, C., Shaver, G.R., 2012. Seasonal patterns of carbon dioxide and water fluxes in three representative tundra ecosystems in northern Alaska. *Ecosphere* 3 (1), <http://dx.doi.org/10.1890/ES11-00202>.
- Fisher, J.B., Sikka, M., Oechel, W.C., et al., 2014. Carbon cycle uncertainty in the Alaskan Arctic. *Biogeosci. Discuss.* 11, 2887–2932, <http://dx.doi.org/10.5194/bgd-11-2887-2014>.
- Frank, J.M., Massman, W.J., Ewers, B.E., 2013. Underestimates of sensible heat flux due to vertical velocity measurement errors in non-orthogonal sonic anemometers. *Agric. Forest Meteorol.* 171, 72–81.
- Fratini, G., McDermitt, D.K., Papale, D., 2014. Eddy-covariance flux errors due to biases in gas concentration measurements: origins, quantification and correction. *Biogeosciences* 11, 1037–1051, <http://dx.doi.org/10.5194/bg-11-1037-2014>.
- Gažovič, M., Forbrich, I., Jäger, D.F., Kutzbach, L., Wille, C., Wilmking, M., 2013. Hydrology-driven ecosystem respiration determines the carbon balance of a boreal peatland. *Sci. Total Environ.* 463, 675–682.
- Gash, J.H.C., Culf, A.D., 1996. Applying linear de-trend to eddy correlation data in real time. *Boundary Layer Meteorol.* 79, 301–306.
- Goulden, M.L., Winston, G.C., McMillan, A.M.S., Litvak, M.E., Read, E.L., Rocha, A.V., Elliot, J.R., 2006. An eddy covariance mesonet to measure the effect of forest age on land-atmosphere exchange. *Global Change Biol.* 12, 2146–2162.
- Grelle, A., Burba, G., 2007. Fine-wire thermometer to correct CO₂ fluxes by open-path analyzers for artificial density fluctuations. *Agric. Forest Meteorol.* 147 (1), 48–57.
- Hanis, K.L., Tenuta, M., Amiro, B.D., Papakyriakou, T.N., 2013. Seasonal dynamics of methane emissions from a subarctic fen in the Hudson Bay Lowlands. *Biogeosciences* 10 (7), 4465–4479.
- Haslwanter, A., Hammerle, A., Wohlfahrt, G., 2009. Open-path vs. closed-path eddy covariance measurements of the net ecosystem carbon dioxide and water vapor exchange: a long-term perspective. *Agric. Forest Meteorol.* 149 (2), 291–302.
- Hollinger, D.Y., Richardson, A.D., 2005. Uncertainty in eddy covariance measurements and its application to physiological models. *Tree Physiol.* 25 (7), 873–885.
- Horst, T.W., Lenschow, D.H., 2009. Attenuation of scalar fluxes measured with spatially-displaced sensors. *Boundary-Layer Meteorol.* 130 (2), 275–300.
- IPCC, 2007. *Climate Change 2007: The Physical Science Basis. Contribution of Working Group I to the Fourth Assessment Report of the Intergovernmental Panel on Climate Change*. In: Solomon, S., Qin, D., Manning, M., Chen, Z., Marquis, M., Averyt, K.B., Tignor, M., Miller, H.L. (Eds.). Cambridge University Press, Cambridge, United Kingdom and New York, NY, USA.
- Ibrom, A., Dellwik, E., Flyvbjerg, H., Jensen, N.O., Pilegaard, K., 2007. Strong low-pass filtering effects on water vapor flux measurements with closed-path eddy correlation systems. *Agric. Forest Meteorol.* 147, 140–156.
- Iwata, H., Kosugi, Y., Ono, K., Mano, M., Sakabe, A., Miyata, A., Takahashi, K., 2014. Cross-validation of open-path and closed-path eddy-covariance techniques for observing methane fluxes. *Boundary Layer Meteorol.* 151, 95–118, <http://dx.doi.org/10.1007/s10546-013-9890-2>.
- Järvi, L., Mammarella, I., Eugster, W., Ibrom, A., Siivola, E., Dellwik, E., Keronen, P., Burba, G., Vesala, T., 2009. Comparison of net CO₂ fluxes measured with open- and closed-path infrared gas analyzers in an urban complex environment. *Boreal Environ. Res.* 14, 499–514.
- Jackowicz-Korczynski, M., Christensen, T.R., Backstrand, K., Crill, P., Friborg, T., Mastepanov, M., Strom, L., 2010. Annual cycle of methane emission from a subarctic peatland. *J. Geophys. Res.* 115 (G02009), <http://dx.doi.org/10.1029/2008jg000913>.
- Kochendorfer, J.P., Meyers, T.P., Frank, J.M., Massman, W.J., Heuer, M.W., 2012. How well can we measure the vertical wind speed? Implications for fluxes of energy and mass. *Boundary Layer Meteorol.* 145 (2), 383–398.
- Kutzbach, L., Wille, C., Pfeiffer, E.-M., 2007. The exchange of carbon dioxide between wet arctic tundra and the atmosphere at the Lena River Delta, Northern Siberia. *Biogeosciences* 4, 869–890.
- Kwon, H.J., Oechel, W.C., Zulueta, R.C., Hastings, S.J., 2006. Effects of climate variability on carbon sequestration among adjacent wet sedge tundra and moist tussock tundra ecosystems. *J. Geophys. Res.-Biogeosci.* 111, 2005–2012.
- Lüers, J., Westermann, S., Piel, K., Boike, J., 2014. Annual CO₂ budget and seasonal CO₂ exchange signals at a High Arctic permafrost site on Spitsbergen, Svalbard archipelago. *Biogeosciences* 11 (22), 6307–6322.
- Lee, X., Black, T.A., Novak, M.D., 1994. Comparison of flux measurements with open- and closed-path gas analyzers above an agricultural field and a forest floor. *Boundary Layer Meteorol.* 67 (1–2), 195–202.
- Lekakis, I.C., Adrian, R.J., Jones, B.G., 1989. Measurement of velocity vectors with orthogonal and non-orthogonal triple-sensor probes. *Exp. Fluids* 7, 228–240.
- Lenschow, D.H., Raupach, M.R., 1991. The attenuation of fluctuations in scalar concentrations through sampling tubes. *J. Geophys. Res.-Atmos.* 96 (D8), 15259–15268.
- Leuning, R., Judd, M.J., 1996. The relative merits of open- and closed-path analysers for measurement of eddy fluxes. *Global Change Biol.* 2 (3), 241–253.
- Leuning, R., King, K.M., 1992. Comparison of eddy-covariance measurements of CO₂ fluxes by open- and closed-path CO₂ analyzers. *Boundary Layer Meteorol.* 59, 297–311.
- Loescher, H.W., Oecheltree, T., Tanner, B., et al., 2005. Comparison of temperature and wind statistics in contrasting environments among different sonic anemometer-thermometers. *Agric. Forest Meteorol.* 133 (1), 119–139.
- Mammarella, I., Launiainen, S., Gronholm, T., Keronen, P., Pumpanen, J., Rannik, Ü., Vesala, T., 2009. Relative humidity effect on the high-frequency attenuation of water vapor flux measured by a closed-path eddy covariance system. *J. Atmos. Oceanic Technol.* 26, 1856–1866.
- Massman, W.J., 1991. The attenuation of concentration fluctuations in turbulent flow through a tube. *J. Geophys. Res.* 96, 15269–15273.
- Massman, W.J., 2000. A simple method for estimating frequency response corrections for eddy-covariance systems. *Agric. Forest Meteorol.* 104, 185–198.
- Mastepanov, M., Sigsgaard, C., Dlugokencky, E.J., Houweling, S., Ström, L., Tamstorf, M.P., Christensen, T.R., 2008. Large tundra methane burst during onset of freezing. *Nature* 456 (7222), 628–630.
- Mastepanov, M., Sigsgaard, C., Tagesson, H.T., Ström, L., Tamstorf, M.P., Lund, M., Christensen, T.R., 2013. Revisiting factors controlling methane emissions from high-Arctic tundra. *Biogeosciences* 10 (7), 5139–5158.
- Mauder, M., Foken, T., 2006. Impact of post-field data processing on eddy covariance flux estimates and energy balance closure. *Meteorol. Z.* 15, 597–609.
- Mauder, M., Oncley, S.P., Vogt, R., Weidinger, T., Ribeiro, L., Bernhofer, C., Foken, T., Kohsiek, W., De Bruin, H.A.R., Liu, H., 2007. The energy balance experiment EBEX-2000. Part II: intercomparison of eddy-covariance sensors and post-field data processing methods. *Boundary Layer Meteorol.* 123 (1), 29–54.

- McDermitt, D., Burba, G., Xu, L., et al., 2011. A new low-power, open-path instrument for measuring methane flux by eddy covariance. *Appl. Phys. B*, <http://dx.doi.org/10.1007/s00340-010-4307-0>.
- Melton, J.R., Wania, R., Hodson, E.L., et al., 2013. Present state of global wetland extent and wetland methane modelling: conclusions from a model intercomparison project (WETCHIMP). *Biogeosciences* 10, 753–788.
- Moncrieff, J.B., Massheder, J.M., de Bruin, H., et al., 1997. A system to measure surface fluxes of momentum, sensible heat, water vapor and carbon dioxide. *J. Hydrol.* 188–189, 589–611.
- Moncrieff, J.B., Clement, R., Finnigan, J., Meyers, T., 2004. Averaging, detrending and filtering of eddy covariance time series. In: Lee, X., Massman, W.J., Law, B.E. (Eds.), *Handbook of Micrometeorology: a Guide for Surface Flux Measurements*. Kluwer Academic, Dordrecht, pp. 7–31.
- Mullier, S.V., Racoviteanu, A.E., Walker, D.A., 1999. Landsat MSS-derived land-cover map of northern Alaska: extrapolation methods and a comparison with photo-interpreted and AVHRR-derived maps. *Int. J. Remote Sens.* 20, 2921–2946.
- Nakai, T., Shimoyama, K., 2012. Ultrasonic anemometer angle of attack errors under turbulent conditions. *Agric. Forest Meteorol.* 162, 14–26.
- Nakai, T., van der Molen, M.K., Gash, J.H.C., Kodama, Y., 2006. Correction of sonic anemometer angle of attack errors. *Agric. Forest Meteorol.* 136, 19–30, <http://dx.doi.org/10.1016/j.agrformet.2006.01.006>.
- Nakai, T., Iwata, H., Harazono, Y., 2011. Importance of mixing ratio for a long-term CO₂ flux measurement with a closed-path system. *Tellus B* 63 (3), 302–308.
- Nakai, T., Kim, Y., Busey, R.C., et al., 2013. Characteristics of evapotranspiration from a permafrost black spruce forest in interior Alaska. *Polar Sci.* 7, 136–148.
- Nakai, T., Iwata, H., Harazono, Y., Ueyama, M., 2014. An inter-comparison between Gill and Campbell sonic anemometers. *Agric. Forest Meteorol.* 195, 123–131.
- Oechel, W.C., Laskowski, C.A., Burba, G., Gioli, B., Kalhori, A.A.M., 2014. Annual patterns and budget of CO₂ flux in an Arctic tussock tundra ecosystem. *J. Geophys. Res.-Biogeosci.* 119, <http://dx.doi.org/10.1002/2013JG002431>.
- Parmentier, F.J.W., van Huissteden, J., van der Molen, M.K., Dolman, A.J., Schaepman-Strub, G., Karsanaev, S.A., Maximov, T.C., 2011. Spatial and temporal dynamics in eddy covariance observations of methane fluxes at a tundra site in northeastern Siberia. *J. Geophys. Res.* 116, G03016, <http://dx.doi.org/10.1029/2010JG001637>.
- Peltola, O., Mammarella, I., Haapanala, S., Burba, G., Vesala, T., 2013. Field intercomparison of four methane gas analyzers suitable for eddy covariance flux measurements. *Biogeosciences* 10, 3749–3765.
- Raynolds, M.K., Walker, D.A., Maier, H.A., 2005. Plant community-level mapping of arctic Alaska based on the Circumpolar Arctic Vegetation Map. *Phytocoenologia* 35 (4), 821–848.
- Reichstein, M., Falge, E., Baldocchi, D., et al., 2005. On the separation of net ecosystem exchange into assimilation and ecosystem respiration: review and improved algorithm. *Global Change Biol.* 11, 1–11, <http://dx.doi.org/10.1111/j.1365-2486.2005.001002.x>.
- Rinne, J., Riutta, T., Pihlatie, M., et al., 2007. Annual cycle of methane emission from a boreal fen measured by the eddy covariance technique. *Tellus* 59B, 449–457.
- Runkle, B.R.K., Wille, C., Gazovic, M., Kutzbach, L., 2012. Attenuation correction procedures for water vapour fluxes from closed-path eddy-covariance systems. *Boundary-Layer Meteorol.* 142, 401–423.
- Sachs, T., Wille, C., Boike, J., Kutzbach, L., 2008. Environmental controls on ecosystem-scale CH₄ emission from polygonal tundra in the Lena River Delta, Siberia. *J. Geophys. Res.-Biogeosci.* 113, 1395–1408.
- Skelly, B.T., Miller, D.R., Meyer, T.H., 2002. Triple-hot-film anemometer performance in CASES-99 and a comparison to sonic anemometer measurements. *Boundary Layer Meteorol.* 105, 275–304.
- Song, W., Wang, H., Wang, G., Chen, L., Jin, Z., Zhuang, Q., He, J.-S., 2015. Methane emissions from an alpine wetland on the Tibetan Plateau: neglected but vital contribution of non-growing season. *J. Geophys. Res.-Biogeosci.*, <http://dx.doi.org/10.1002/2015JG003043>.
- Sturtevant, C.S., Oechel, W.C., Zona, D., Kim, Y., Emerson, C.E., 2012. Soil moisture control over autumn season methane flux, Arctic Coastal Plain of Alaska. *Biogeosciences* 9, 1423–1440.
- Tammelin, B., Cavaliere, M., Kimura, S., Morgan, C., 1998. Ice free anemometers. *BOREAS* IV 31 March–2 April 1998, Hetta, Finland, pp. 239–252.
- Taylor, J.R., 1997. *Error Analysis; The Study of Uncertainties in Physical Measurements*, 2nd ed. University Science Books, Sausalito, CA, US.
- Ueyama, M., Hirata, R., Mano, M., et al., 2012. Influences of various calculation options on heat, water and carbon fluxes determined by open- and closed-path eddy covariance methods. *Tellus B*, <http://dx.doi.org/10.3402/tellusb.v64i0.19048>.
- Ueyama, M., Iwata, H., Harazono, Y., Euskirchen, E.S., Oechel, W.C., Zona, D., 2013. Growing season and spatial variations of carbon fluxes of Arctic and boreal ecosystems in Alaska. *Ecol. Appl.* 23, 1798–1816.
- Vickers, D., Mahrt, L., 1997. Quality control and flux sampling problems for tower and aircraft data. *J. Atmos. Oceanic Technol.* 14, 512–526.
- Webb, E.K., Pearman, G.I., Leuning, R., 1980. Correction of flux measurements for density effects due to heat and water vapor transfer. *Q. J. R. Meteorolog. Soc.* 106, 85–100.
- Wilczak, J.M., Oncley, S.P., Stage, S.A., 2001. Sonic anemometer tilt correction algorithms. *Boundary Layer Meteorol.* 99, 127–150.
- Wille, C., Kutzbach, L., Sachs, T., Wagner, D., Pfeiffer, E., 2008. Methane emission from Siberian arctic polygonal tundra: eddy covariance measurements and modeling. *Global Change Biol.* 14 (6), 1395–1408.
- Zona, D., Oechel, W.C., Kochendorfer, J., et al., 2009. Methane fluxes during the initiation of a large-scale water table manipulation experiment in the Alaskan Arctic tundra. *Global Biogeochem. Cycles* 23 (2), <http://dx.doi.org/10.1029/2009GB003487>.
- Zona, D., Oechel, W.C., Peterson, K.M., Clements, R.J., Paw, U.K.T., Ustin, S.L., 2010. Characterization of the carbon fluxes of a vegetated drained lake basin chronosequence on the Alaskan Arctic Coastal Plain. *Global Change Biol.* 16, 1870–1882, <http://dx.doi.org/10.1111/j.1365-2486.2009.02107>.
- Zona, D., Oechel, W.C., Richards, J.H., Hastings, S., Kopetz, I., Ikawa, H., Oberbauer, S., 2011. Light-stress avoidance mechanisms in a Sphagnum-dominated wet coastal Arctic tundra ecosystem in Alaska. *Ecology* 92, 633–644, <http://dx.doi.org/10.1890/10-0822.1>.
- Zona, D., Lipson, D.A., Paw, U.K.T., Oberbauer, S.F., Olivas, P., Gioli, B., Oechel, W.C., 2012. Increased CO₂ loss from vegetated drained lake tundra ecosystems due to flooding. *Global Biogeochem. Cycles* 26 (GB2013), <http://dx.doi.org/10.1029/2011GB004037>.
- Zona, D., Lipson, D.A., Richards, J.H., et al., 2014. Delayed responses of an Arctic ecosystem to an extreme summer: impacts on net ecosystem exchange and vegetation functioning. *Biogeosciences* 11 (20), 5877–5888.
- Zona, D., Gioli, B., Commane, R., Lindaas, J., Wofsy, S.C., Miller, C.E., Dinardo, S.J., Dengel, S., Sweeney, C., Karion, A., Chang, R.Y.-W., Henderson, J.M., Murphy, P.C., Goodrich, J.P., Moreaux, V., Liljedahl, A., Watts, J.D., Kimball, J.S., Lipson, D.A., Oechel, W.C., 2016. Cold season emission dominate the Arctic tundra methane budget. *Proc. Natl. Acad. Sci.* 113 (1), 40–45.

1 **Appendix A. Supplementary Material**

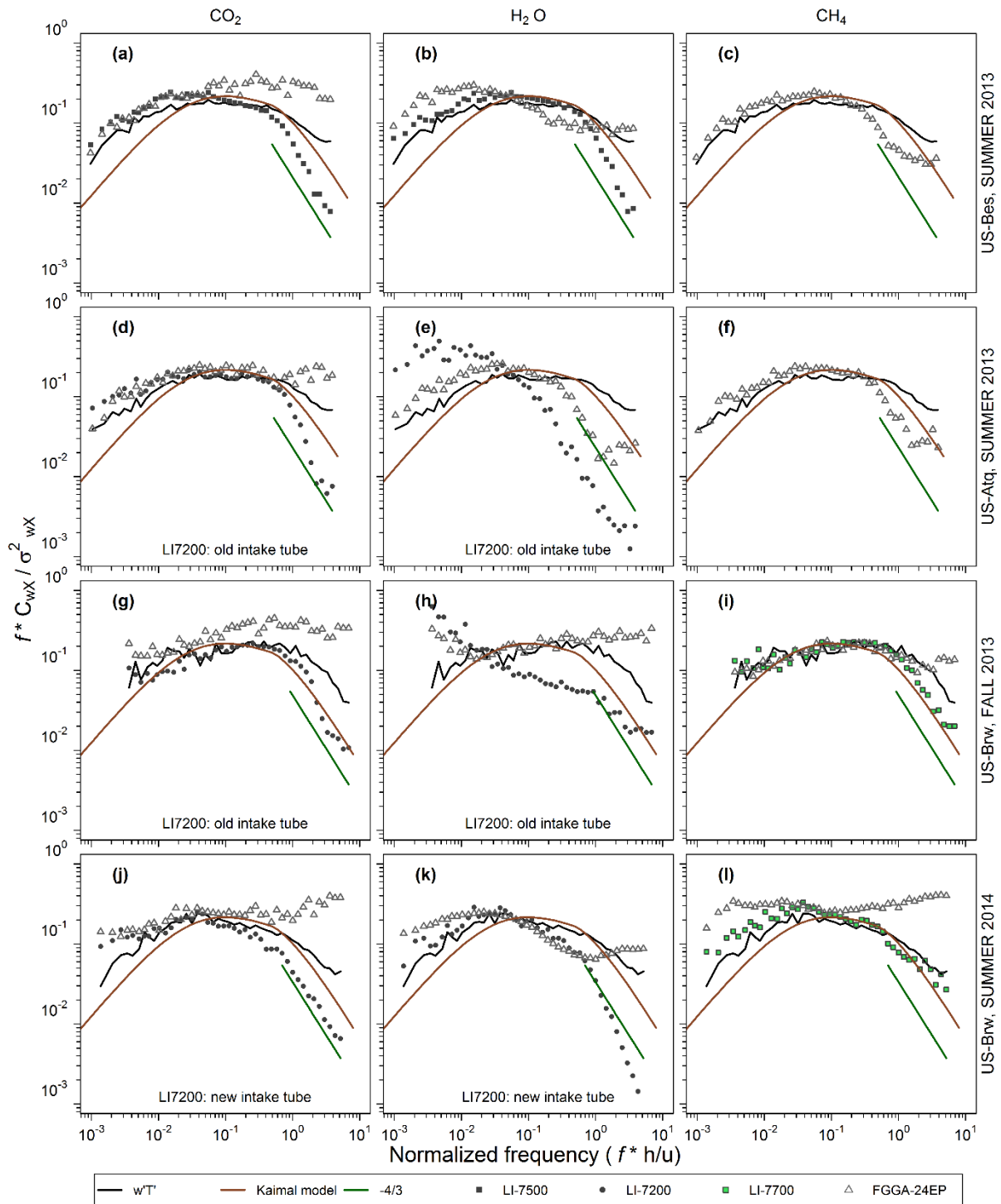
2

3



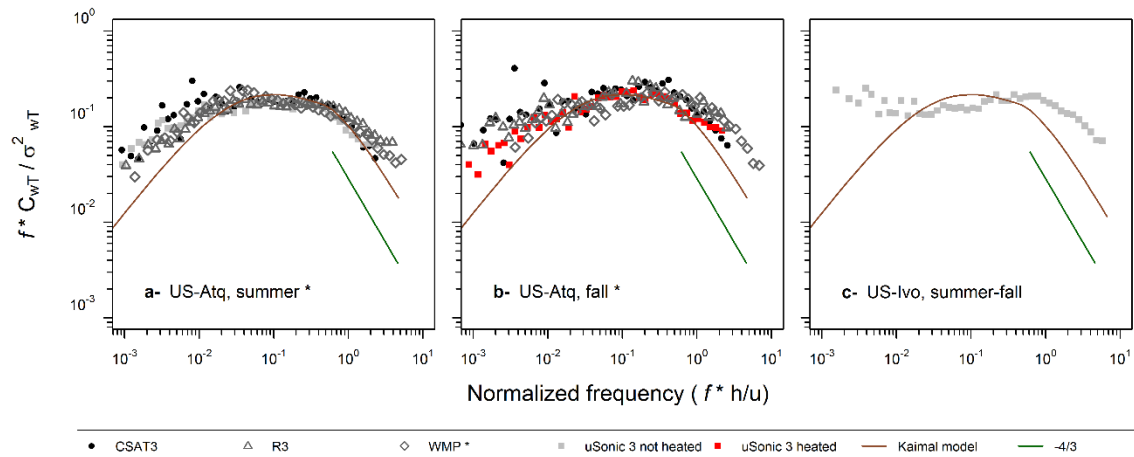
5 **Figure S1.** Comparisons of 30-min average LE between closed and (en)closed-path sensors
6 ATQ. The (en)closed-path LI-7200 was equipped with an unheated tube and rain cup of the
7 larger pre-2013 design ($n = 2500$), which were subsequently replaced by smaller designs in
8 mid-2014 ($n = 3171$), greatly reducing attenuation of the H_2O signal and improving
9 comparisons with the closed-path LGR-FGGA-24EP with heated tubing.

10



11
 12
 13
 14
 15
 16
 17
 18
 19
 20

Figure S2. Daytime normalized binned-ensemble-averaged flux cospectra of CO₂ (a, d, g, j), H₂O (b, e, h, k) and CH₄ (c, f, i, l) plotted versus normalized frequency for three experimental sites during common periods when data from different measurements systems were available at the same time. Kaimal's model for unstable and neutral conditions and -4/3 slope are also shown for each site to provide a reference as to what should be expected for a high-frequency drop-off. The x-axis in each plot is the non-dimensional frequency (f), normalized by measurement height (h) and horizontal wind speed (u).



21
 22 **Figure S3.** Daytime normalized binned-ensemble-averaged w'T' cospectra plotted versus
 23 normalized frequency for three sonic anemometers during periods when data from different
 24 anemometers were available at the same time: (a) ATQ between the 15 August and the 27
 25 August 2013; (b). ATQ between 8 October and 31 October 2013; and (c) IVO between the 8
 26 October and 31 October 2013. Kaimal model for unstable and neutral conditions and -4/3
 27 damping slope are also shown for each site to provide a reference as to what should be
 28 expected for a high-frequency drop-off. * indicates that the Gill WMP used in CMDL has
 29 been added as for information purpose. The x-axis in each plot is the non-dimensional
 30 frequency (f), normalized by measurement height (h) and horizontal wind speed (u).

31
 32
 33